Dear author,

Please note that changes made in the online proofing system will be added to the article before publication but are not reflected in this PDF.

We also ask that this file not be used for submitting corrections.

Journal of Quantitative Spectroscopy & Radiative Transfer ■ (■■■■) ■■■–■■■

Contents lists available at ScienceDirect

Journal of Quantitative Spectroscopy & Radiative Transfer

journal homepage: www.elsevier.com/locate/jqsrt

Assessment of Tikhonov-type regularization methods for solving atmospheric inverse problems

Jian Xu*, Franz Schreier, Adrian Doicu, Thomas Trautmann

German Aerospace Center (DLR), Remote Sensing Technology Institute (IMF), 82234 Oberpfaffenhofen, Germany

ARTICLE INFO

Article history:
Received 25 May 2016
Received in revised form
3 August 2016
Accepted 4 August 2016

Keywords:
Atmospheric inverse problems
Direct and iterative Tikhonov-type regularization
Regularization parameter selection methods

ABSTRACT

Inverse problems occurring in atmospheric science aim to estimate state parameters (e.g. temperature or constituent concentration) from observations. To cope with nonlinear ill-posed problems, both direct and iterative Tikhonov-type regularization methods can be used. The major challenge in the framework of direct Tikhonov regularization (TR) concerns the choice of the regularization parameter λ, while iterative regularization methods require an appropriate stopping rule and a flexible λ-sequence.

In the framework of TR, a suitable value of the regularization parameter can be generally determined based on a priori, a posteriori, and error-free selection rules. In this study, five practical regularization parameter selection methods, i.e. the expected error estimation (EEE), the discrepancy principle (DP), the generalized cross-validation (GCV), the maximum likelihood estimation (MLE), and the L-curve (LC), have been assessed. As a representative of iterative methods, the iteratively regularized Gauss–Newton (IRGN) algorithm has been compared with TR. This algorithm uses a monotonically decreasing λ-sequence and DP as an a posteriori stopping criterion.

Practical implementations pertaining to retrievals of vertically distributed temperature and trace gas profiles from synthetic microwave emission measurements and from real far infrared data, respectively, have been conducted. Our numerical analysis demonstrates that none of the parameter selection methods dedicated to TR appear to be perfect and each has its own advantages and disadvantages. Alternatively, IRGN is capable of producing plausible retrieval results, allowing a more efficient manner for estimating λ.

1. Introduction

Temporal and spatial knowledge of molecular concentrations in Earth's atmosphere is important for the scientific community to study the behavior of ozone depletion and air pollution. Temperature is a critical parameter for chemical, dynamical, and radiative processes in the atmosphere and its change is highly correlated with some on-going atmospheric phenomena (e.g. climate change). These atmospheric quantities can be derived by remotely measuring emitted thermal radiation in an appropriate spectral range.

Inverse problems encountered in atmospheric science aim to estimate these atmospheric state parameters (temperature and concentration profiles) from collected measurements. These problems are inherently ill-posed in the sense that the noise in the measurements leads to large errors in the estimate. To stabilize the problem and to attain a solution with physical meaning, additional constraints have to be introduced during the inversion, a process which is referred to as regularization. In this regard, it provides the necessary impetus to investigate the design and robustness of inversion algorithms.

* Corresponding author.
E-mail address: jian.xu@dlr.de (J. Xu).

http://dx.doi.org/10.1016/j.jqsrt.2016.08.003
0022-4073/

A direct regularization method, namely Tikhonov regularization (TR) [1], has been widely used for stabilizing ill-posed inverse problems. However, in the presence of measurement errors, the regularized solution frequently fails to possess optimal accuracy if the regularization parameter is not chosen properly. Engl et al. [2], Vogel [3], and Doicu et al. [4] have introduced and discussed several classical regularization parameter selection methods. Some new methods have been proposed and applied in atmospheric science and other fields, e.g. [5–9]. Still, it remains unclear if there would exist an infallible parameter selection method. Only a limited number of studies focus on performance comparisons of different techniques for estimating the regularization parameter, e.g. [10,11]. It can be foreseen that many data analyses would certainly benefit from these studies by enhancing the quality of retrieval products.

Finding a global minimizer of the Tikhonov function is computationally expensive, and in particular, determining an appropriate regularization parameter can be time-consuming. Iterative regularization methods as an alternative to direct regularization methods can reduce the amount of effort required to choose the regularization parameter. However, the stopping criterion of the iterative process has to be carefully chosen in order to avoid an uncontrolled explosion of the noise error.

Measurements of vertically distributed atmospheric parameters are primarily obtained by remote sensing techniques from diverse platforms. This study places an emphasis on exploiting the thermal emission emitted by the atmosphere in the infrared and microwave regions.

For example, the airborne Microwave Temperature Profiler (MTP) [12,13], initially developed at NASA's Jet Propulsion Laboratory (JPL), measures natural thermal emission from oxygen lines at a selection of frequencies around 55–60 GHz by scanning from near nadir to near zenith in the flight direction. Recently, the MTP instrument has been flown on the HALO research aircraft operated by DLR. These airborne measurements help to better understand the vertical state around the upper troposphere and lower stratosphere (UTLS).

TELIS (TErahertz and submillimeter LImb Sounder) [14] is a cryogenic multi-channel heterodyne spectrometer designed to investigate atmospheric chemistry and dynamics focusing on the stratosphere (10–40 km). The instrument was mounted on a balloon gondola together with the balloon-version of MIPAS (Michelson Interferometer for Passive Atmospheric Sounding) [15] and mini-DOAS (Differential Optical Absorption Spectrometer). This combination has accomplished four scientific flights over Kiruna, Sweden and Timmins, Canada between 2009 and 2014. The principal objective of these balloon campaigns has been to measure the time-dependent chemistry of chlorine (Cl) and bromine (Br), and to achieve the closure of chemical families (NO_y, Cl_y, Br_y, HO_x) inside the polar vortex.

The goal of this work is to present various Tikhonov-type regularization schemes for tackling ill-posed inverse problems arising from atmospheric remote sensing and to examine their numerical performances in estimating atmospheric temperature and concentration profiles from spectral measurements. We explain the theory of regularized nonlinear inversion in Section 2. Five regularization parameter selection methods dedicated to TR are described in Section 2.1, and an iterative regularization method together with its stopping rule is introduced in Section 2.2. Temperature retrievals from synthetic airborne MTP data with different noise configurations are analyzed in Section 3, while in Section 4, trace gas retrievals from real TELIS data are discussed in terms of accuracy and efficiency. The emphasis pertains to the selection of an appropriate regularization parameter by using different strategies and to the comparison of direct and iterative regularization methods. Finally, Section 5 gives an outline of our findings.

2. Regularization for solving nonlinear problems

Most inverse problems in atmospheric remote sensing are nonlinear and can be expressed by the equation $\boldsymbol{F}(\boldsymbol{x})=\boldsymbol{y}$, where for discrete problems, $\boldsymbol{F}:\mathbb{R}^n\to\mathbb{R}^m$ is the forward model, $\boldsymbol{x}\in\mathbb{R}^n$ is the state vector, and $\boldsymbol{y}\in\mathbb{R}^m$ is the "exact" measurement vector. In practice, $\boldsymbol{y}$ cannot be known precisely; we have only its "perturbed" version $\boldsymbol{y}^\delta=\boldsymbol{y}+\boldsymbol{\delta}\in\mathbb{R}^m$, where $\boldsymbol{\delta}$ is the measurement noise, and for which the following estimate holds: $\|\boldsymbol{y}^\delta-\boldsymbol{y}\|^2=\Delta^2$ with Δ being the noise level. In this study, the measurement vector $\boldsymbol{y}^\delta$ is a concatenation of radiances or brightness temperatures received by the instrument, whereas the unknown state vector $\boldsymbol{x}$ stands for the discretized vertical temperature or concentration profiles (and optionally of some auxiliary parameters) to be reconstructed based on given data and some a priori knowledge.

By imposing the smoothness constraint, the regularization method converts an ill-posed problem into a well-posed one. In the framework of TR, the regularized solution $\boldsymbol{x}_\lambda$ minimizes the objective function

$$\mathcal{F}(\boldsymbol{x})=\|\boldsymbol{F}(\boldsymbol{x})-\boldsymbol{y}^\delta\|^2+\lambda\|\mathbf{L}(\boldsymbol{x}-\boldsymbol{x}_\mathrm{a})\|^2. \tag{1}$$

The residual term $\|\boldsymbol{F}(\boldsymbol{x})-\boldsymbol{y}^\delta\|^2$ quantifies the goodness of fit, whereas the penalty term $\|\mathbf{L}(\boldsymbol{x}-\boldsymbol{x}_\mathrm{a})\|^2$ measures the regularity of the solution, where $\mathbf{L}$ and λ are the regularization matrix and the regularization parameter, respectively, and $\boldsymbol{x}_\mathrm{a}$ is the a priori state vector. In principle, minimization of $\mathcal{F}(\boldsymbol{x})$ aims to seek $\boldsymbol{x}_\lambda$ for reaching an optimal compromise between the residual term and the penalty term. Therefore, the regularization strength is constrained by the form of $\mathbf{L}$ and the size of λ.

The minimization problem can be solved by the Gauss–Newton algorithm which comprises a linearization of the forward model $\boldsymbol{F}$ about the current iterate $\boldsymbol{x}_{\lambda,i}$. The next iterate is then given by

$$\boldsymbol{x}_{\lambda,i+1}=\boldsymbol{x}_\mathrm{a}+\mathbf{K}_{\lambda,i}^\dagger\left(\boldsymbol{y}^\delta-\boldsymbol{F}(\boldsymbol{x}_{\lambda,i})+\mathbf{K}_i(\boldsymbol{x}_{\lambda,i}-\boldsymbol{x}_\mathrm{a})\right), \tag{2}$$

where

$$\mathbf{K}_{\lambda,i}^\dagger=\left(\mathbf{K}_i^T\mathbf{K}_i+\lambda\mathbf{L}^T\mathbf{L}\right)^{-1}\mathbf{K}_i^T \tag{3}$$

is the regularized generalized inverse (also known as the gain matrix [16]) at the iteration step i and $\mathbf{K}_i\in\mathbb{R}^{m\times n}$ is the Jacobian matrix of $\boldsymbol{F}$ at $\boldsymbol{x}_i$.

Please cite this article as: Xu J, et al. Assessment of Tikhonov-type regularization methods for solving atmospheric inverse problems. J Quant Spectrosc Radiat Transfer (2016), http://dx.doi.org/10.1016/j.jqsrt.2016.08.003

Basically, **L** can be the identity matrix, a discrete approximation of a derivative operator, or the Cholesky factor of an a priori profile covariance matrix (e.g. climatological knowledge). Further discussions about the construction of the regularization matrix are beyond the scope of this work, as we only focus on the design of regularization parameter selection methods. Instabilities resulting from a weak regularization can be expected when λ is chosen too small. On the contrary, nearly no connection with the original problem would exist in the case of a strong regularization when λ is chosen too large. It is worth mentioning that the following regularization methods are formulated in a semi-stochastic setting and that, under the assumption that $\boldsymbol{\delta}$ is a discrete white noise with variance σ^2, the noise level is evaluated as $\Delta^2 = m\sigma^2$.

According to [16], the degree of nonlinearity of the objective function (1) is determined by the spectral characteristics of $\boldsymbol{y}^\delta$ (e.g. spectral range, units, and noise) and the unknowns $\boldsymbol{x}$. In a stochastic framework, the degree of nonlinearity can be estimated by comparing the forward model with the linearized forward model within the a priori variability. The size of the linearization error is represented as

$$\boldsymbol{R} = \boldsymbol{F}(\boldsymbol{x}) - \boldsymbol{F}(\boldsymbol{x}_\mathrm{a}) - \mathbf{K}(\boldsymbol{x}_\mathrm{a})(\boldsymbol{x} - \boldsymbol{x}_\mathrm{a}) \tag{4}$$

and can be used to calculate the so-called nonlinearity parameter:

$$\epsilon^2_{\mathrm{lin},k} = \frac{\left\|\boldsymbol{R}(\boldsymbol{x}_\mathrm{a} \pm \boldsymbol{c}_k)\right\|^2}{m\sigma^2}, \tag{5}$$

where the vectors $\boldsymbol{c}_k$ denote the error patterns of the a priori covariance. In case that $\epsilon_{\mathrm{lin},k} \le 1$ for all k, this particular problem is characterized by a small linearization error and can be considered to be linear within the assumed range of variation in $\boldsymbol{x}_\mathrm{a}$.

2.1. Regularization parameter selection methods

For direct Tikhonov regularization, a reliable approximation $\boldsymbol{x}_\lambda$ of the true state $\boldsymbol{x}_\mathrm{t}$ counts on a proper selection of the regularization parameter λ. In general, selection criteria with variable or constant λ can be employed. In the former case, λ is estimated by a particular selection method at each iteration step. In our analysis, the latter is considered, i.e. the minimization of the objective function (1) is performed with a single λ and this procedure is repeated several times with different values of λ.

According to Engl et al. [2], an appropriate regularization parameter can be selected by using a priori, a posteriori, and error-free selection rules. We present below five parameter selection methods based on these rules.

2.1.1. A priori parameter selection rule

Essentially, an a priori parameter selection method relies on the knowledge of Δ. In the so-called expected error estimation (EEE) method, the optimal regularization parameter λ_opt is chosen as the minimizer of the expected error:

$$\lambda_\mathrm{opt} = \arg\min_\lambda \mathcal{E}\left[\|\boldsymbol{e}_\lambda\|^2\right], \tag{6}$$

where

$$\mathcal{E}\left[\|\boldsymbol{e}_\lambda\|^2\right] = \|\boldsymbol{e}_\mathrm{s}\|^2 + \mathcal{E}\left[\left\|\boldsymbol{e}_\mathrm{y}\right\|^2\right] + \left\|\boldsymbol{e}_\mathrm{b}\right\|^2 + \|\boldsymbol{e}_\mathrm{c}\|^2. \tag{7}$$

On the right side of Eq. (7), the smoothing error $\boldsymbol{e}_\mathrm{s}$ is estimated by

$$\boldsymbol{e}_\mathrm{s} = (\mathbf{A} - \mathbf{I}_n)(\boldsymbol{x}_\mathrm{t} - \boldsymbol{x}_\mathrm{a}), \tag{8}$$

where $\mathbf{A} = \mathbf{K}_\lambda^\dagger \mathbf{K}$ is the averaging kernel matrix, and hence the deviation of **A** from the identity matrix $\mathbf{I}_n$ characterizes the smoothing error. In practice, regularization degrades the vertical resolution, that is reflected by the peak value of **A** at an altitude level and the full width at half maximum of this peak. The trace of **A** yields the degree of freedom for signal (DOFS) that is interpreted as a measure of the effective information content. As the diagonal values of **A** become smaller with increasing λ, the DOFS turns out to be a decreasing function of λ.

The expected value of the noise error $\boldsymbol{e}_\mathrm{y}$ is given by

$$\mathcal{E}\left[\left\|\boldsymbol{e}_\mathrm{y}\right\|^2\right] = \sigma^2 \,\mathrm{trace}\left(\mathbf{K}_\lambda^\dagger \mathbf{K}_\lambda^{\dagger T}\right). \tag{9}$$

It is well known that uncertainties in atmospheric profiles used in the forward model or instrument parameters can cause additional errors in the retrieval. Regarding the forward model error $\boldsymbol{e}_\mathrm{b}$, we use the approximation

$$\boldsymbol{e}_\mathrm{b} = \mathbf{K}_\lambda^\dagger \boldsymbol{\delta}_\mathrm{b} = \mathbf{K}_\lambda^\dagger \mathbf{K}_\mathrm{b} \Delta\boldsymbol{b} \tag{10}$$

$$\boldsymbol{e}_\mathrm{b} \approx \mathbf{K}_\lambda^\dagger (\boldsymbol{F}(\boldsymbol{x}_\mathrm{t}, \boldsymbol{b} + \Delta\boldsymbol{b}) - \boldsymbol{F}(\boldsymbol{x}_\mathrm{t}, \boldsymbol{b})), \tag{11}$$

where $\Delta\boldsymbol{b}$ are the uncertainties in $\boldsymbol{b}$ and $\mathbf{K}_\mathrm{b}$ is the Jacobian matrix with respect to $\boldsymbol{b}$. Similar estimates are used for the instrument model error $\boldsymbol{e}_\mathrm{c}$.

Such a parameter selection strategy does not depend on the actual perturbed data $\boldsymbol{y}^\delta$. In practice, the exact solution is unknown and one can deal with this method in a statistical way. For example, a strategy is to explore a random solution domain where $\boldsymbol{x}_\mathrm{t}$ is supposed to lie, by using the synthetic data $\boldsymbol{x}_{\mathrm{t},j}$, $j = 1,\ldots, M$, with M representing the sample size. The main drawback is that the optimal regularization parameter λ_opt needs to be predicted for each solution sample by repeatedly solving the minimization problem, and therefore, this off-line estimation procedure presumably requires considerable computational burden.

2.1.2. A posteriori parameter selection rule

The selection of the regularization parameter using the a posteriori parameter selection rule depends on both Δ and $\boldsymbol{y}^\delta$. In the discrepancy principle (DP) method [17], the regularization parameter λ is chosen as the solution to the equation

$$\left\|\boldsymbol{r}_\lambda^\delta\right\|^2 = \left\|\boldsymbol{F}(\boldsymbol{x}_\lambda) - \boldsymbol{y}^\delta\right\|^2 = \chi\Delta^2 = \chi m\sigma^2, \tag{12}$$

where $\chi > 1$ is a control parameter. Thus, λ is chosen through a comparison between the residual norm (or discrepancy) $\left\|\boldsymbol{r}_\lambda^\delta\right\|$ and the assumed noise level Δ. Because of its property, this strategy can also be used as a stopping rule in the framework of iterative regularization methods, which will be discussed in Section 2.2.

Please cite this article as: Xu J, et al. Assessment of Tikhonov-type regularization methods for solving atmospheric inverse problems. J Quant Spectrosc Radiat Transfer (2016), http://dx.doi.org/10.1016/j.jqsrt.2016.08.003

2.1.3. Error-free parameter selection rule

An error-free parameter selection method requires only the knowledge of $\boldsymbol{y}^{\delta}$, and not of Δ. Accordingly, these parameter selection methods do not count on the setting in which the inverse problem is formulated. In this study, three error-free parameter selection methods are examined.

In the method of generalized cross-validation (GCV) [18,19], λ is chosen as the minimizer of the GCV function $V(\lambda)$:

$$\lambda_{\mathrm{opt}} = \arg\min_{\lambda} V(\lambda), \tag{13}$$

where

$$V(\lambda) = \frac{m^2 \left\|\boldsymbol{r}_{\lambda}^{\delta}\right\|^2}{\left[\mathrm{trace}\left(\mathbf{I}_m - \mathbf{K}\mathbf{K}_{\lambda}^{\dagger}\right)\right]^2}. \tag{14}$$

The trace term in the denominator stands for the "degree of freedom for noise". This method tries to find the transition point where $\left\|\boldsymbol{r}_{\lambda}^{\delta}\right\|$ changes from a slowly varying function of λ to a rapidly increasing function of λ. Note that Eq. (14) possesses a minimum as $\left\|\boldsymbol{r}_{\lambda}^{\delta}\right\|$ increases with λ.

In the so-called maximum likelihood estimation (MLE) method [19,20], λ is chosen as the minimizer of the maximum likelihood (ML) function $E(\lambda)$:

$$\lambda_{\mathrm{opt}} = \arg\min_{\lambda} E(\lambda), \tag{15}$$

where

$$E(\lambda) = \frac{\boldsymbol{y}_{\lambda}^{T}\left(\mathbf{I}_m - \mathbf{K}\mathbf{K}_{\lambda}^{\dagger}\right)\boldsymbol{y}_{\lambda}}{\sqrt[m]{\det\left(\mathbf{I}_m - \mathbf{K}\mathbf{K}_{\lambda}^{\dagger}\right)}} \tag{16}$$

with $\boldsymbol{y}_{\lambda} = \boldsymbol{y}^{\delta} - \boldsymbol{F}(\boldsymbol{x}_{\lambda}) + \mathbf{K}(\boldsymbol{x}_{\lambda} - \boldsymbol{x}_{\mathrm{a}})$. This selection criterion can be seen as an alternative to the GCV method when the unique minimizer of the GCV function cannot be determined.

The L-curve (LC) method was initially advocated by Hansen [21] and its use for nonlinear problems was explored by Eriksson [22]: the constraint $\left\|\boldsymbol{c}_{\lambda}^{\delta}\right\|^2 = \left\|\mathbf{L}(\boldsymbol{x}_{\lambda} - \boldsymbol{x}_{\mathrm{a}})\right\|^2$ versus the residual $\left\|\boldsymbol{r}_{\lambda}^{\delta}\right\|^2 = \left\|\boldsymbol{F}(\boldsymbol{x}_{\lambda}) - \boldsymbol{y}^{\delta}\right\|^2$ for a range of values of λ is visualized in logarithmic scale. Besides on a log–log scale, the "L" shaped curve can also be examined on a linear scale when the variation of the residual term is very low [23].

According to Hansen and O'Leary [24], the optimal regularization parameter corresponds to the corner of the curve which is the point of maximum curvature:

$$\lambda_{\mathrm{opt}} = \arg\max_{\lambda} \kappa(\lambda), \tag{17}$$

where the curvature function is defined as

$$\kappa(\lambda) = \frac{x''(\lambda)y'(\lambda) - x'(\lambda)y''(\lambda)}{\left[x'(\lambda)^2 + y'(\lambda)^2\right]^{3/2}} \tag{18}$$

with $x(\lambda) = \log\left(\left\|\boldsymbol{r}_{\lambda}^{\delta}\right\|^2\right)$ and $y(\lambda) = \log\left(\left\|\boldsymbol{c}_{\lambda}^{\delta}\right\|^2\right)$. A practical implementation of this method is that a considerable number of discrete points corresponding to different values of λ are needed.

2.2. An iterative regularization method

In the framework of TR, the selection of the regularization parameter may require a vast amount of computational effort. Alternatively, iterative regularization methods can be considered as an efficient option regarding the estimation of the regularization parameter. Here, the number of iterations and the stopping criterion play the role of the regularization parameter and the parameter selection method, respectively.

In this study, we use the iteratively regularized Gauss–Newton (IRGN) method which was originally introduced by Bakushinskii [25]. The regularized solution $\boldsymbol{x}_{\lambda}$ is computed according to Eq. (2), but the regularization parameters are iteration-dependent and are defined as a monotonically decreasing sequence satisfying:

$$r = \frac{\lambda_{i+1}}{\lambda_i}, \quad \lambda_i > 0, \quad \lim_{i\to\infty} \lambda_i = 0, \tag{19}$$

where $r < 1$ represents the ratio of the geometric sequence. Here, we apply $r \geq 0.8$ so that the regularization strength is slowly decreased during the iterative process. For atmospheric inverse problems in the infrared spectral region, the numerical performances of this algorithm with/without bound-constraint on the variables have been analyzed in [26,27].

As compared to direct regularization methods, the main advantage of this method is that an overestimation of the initial value of λ may still produce reasonable retrieval results despite more iteration steps [28]. However, the iterative process has to be stopped after a right number of steps i^* in order to avoid an uncontrolled explosion of the noise error: while the residual decreases as the iteration continues, the error $\left\|\boldsymbol{x}_{\lambda,i} - \boldsymbol{x}_{\mathrm{t}}\right\|$ begins to increase after an initial decay. Theoretically, a priori stopping rules require information on the exact solution, which may not be suitable for real practical problems, whereas a posteriori stopping rules require only available information [29]. A modified version of DP is used here as an a posteriori stopping rule: the stopping index i^* is chosen as

$$\left\|\boldsymbol{F}(\boldsymbol{x}_{\lambda,i^*}) - \boldsymbol{y}^{\delta}\right\|^2 \leq \chi\left\|\boldsymbol{r}^{\delta}\right\|^2 < \left\|\boldsymbol{F}(\boldsymbol{x}_{\lambda,i}) - \boldsymbol{y}^{\delta}\right\|^2, \quad 0 \leq i < i^*, \tag{20}$$

where $\left\|\boldsymbol{r}^{\delta}\right\|$ is the residual norm at the final iteration step and replace the noise level $\Delta^2 = m\sigma^2$ in Eq. (12).

The control parameter χ in Eqs. (12) and (20) can affect the retrieval quality of direct and iterative regularization methods. In general, χ ought to be greater than 1, otherwise the residual norm may not be able to reach the given tolerance. From a mathematical point of view, Engl et al. [2] and Kaltenbacher et al. [29] have claimed that the value of χ should be sufficiently large, or at least greater than 2. However, we have found that values just slightly larger than 1 deliver more plausible retrievals (see Sections 3 and 4). Unfortunately, a quantitative theory to account for this stopping rule has not yet been formulated, though it works well enough in practice.

In order to avoid local minima, the regularization strength is large at the beginning of the iterative process and then it is gradually decreased. The initial value of λ can

Please cite this article as: Xu J, et al. Assessment of Tikhonov-type regularization methods for solving atmospheric inverse problems. J Quant Spectrosc Radiat Transfer (2016), http://dx.doi.org/10.1016/j.jqsrt.2016.08.003

be selected from an inspection of the singular values of the Jacobian matrix **K**.

At first glance, this method looks pretty similar to the method of TR with a variable regularization parameter, but in the IRGN method λ is continuously decreased and the iterative process is terminated by the discrepancy principle rather than configuring the convergence criterion.

2.3. Implementation

As stated previously, the purpose of the retrieval algorithm is to determine the atmospheric parameters which best fit the simulations to the measurements. The main components of the retrieval algorithm are forward modeling, Jacobian evaluation, and iterative fitting.

In our algorithm, the forward model that simulates atmospheric radiative transfer is built on an extensive and modular line-by-line program GARLIC (Generic Atmospheric Radiation Line-by-line Infrared Code) [30]. Infrared/microwave observations obtained by various instruments have been analyzed by retrieval codes which are also adapted from GARLIC [28,31].

A noteworthy feature of the retrieval algorithm is that the Jacobians with respect to the components of the state vector are evaluated by means of algorithmic (or automatic) differentiation (AD) [32,33]. Schreier et al. [34] have proved that AD Jacobians are favorable in terms of algorithmic efficiency, ease of implementation, and accuracy as compared to finite difference Jacobians. In this work, a source-to-source AD tool called TAPENADE [35] was utilized.

The iterative process was carried out in a Tikhonov-type (direct and iterative) regularized nonlinear least squares fitting framework. In order to choose a proper regularization parameter in the framework of TR, all the above-mentioned parameter selection methods have been implemented in the retrieval algorithm. The singular values of the Jacobian matrix were used for determining a range of values of the regularization parameter λ. In Sections 3 and 4, the retrieval quality will be analyzed in terms of the inversion accuracy, goodness of fit, and useful information content which are characterized by the solution error, residual, and DOFS, respectively.

3. Temperature retrieval

To investigate the different regularization schemes presented in Section 2, we considered a temperature retrieval test problem using synthetic MTP data. Each measurement cycle $\boldsymbol{y}^\delta$ typically contains a set of 30 brightness temperatures (in units of K) corresponding to 3 frequencies and 10 viewing angles. Here, the atmospheric temperature profile was retrieved from $\boldsymbol{y}^\delta$ in a spectral interval ranging from about 56 to 59 GHz. The observer altitude was set to 10.0 km.

For the noisy data vector $\boldsymbol{y}_i^\delta = \boldsymbol{y} + \boldsymbol{\delta}_i$ with $i = 1,...,N$, the exact data $\boldsymbol{y}$ were generated for an ensemble of 42 diverse climatological atmospheres [36] (see Fig. 1). Three noise standard deviations σ (0.05, 0.1, 0.2) were considered according to previous in-flight observations. The first six

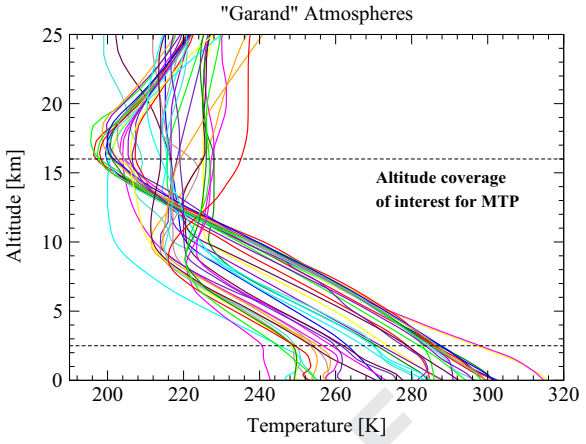

Fig. 1. Temperature profiles of the 42 "Garand" atmospheres. The plotted altitude range refers to the range used for generating $\boldsymbol{y}$. In the original profiles, the top of the atmosphere is always set to 0.1 mb (around 60 km).

Table 1
Degree of nonlinearity quantified by the nonlinearity parameter corresponding to 10 error patterns for the temperature retrieval problem.

Error pattern index	Nonlinearity parameter
1	1.291
2	1.016
3	0.874
4	0.635
5	0.462
6	0.218
7	0.145
8	0.082
9	0.063
10	0.038

profiles are the AFGL standard profiles [37], i.e. tropical (G01), mid-latitude summer and winter (G02 and G03), subarctic summer and winter (G04 and G05), and U.S. standard atmosphere (G06). The remaining 36 profiles are selected from Turner [38].

The exact state vector $\boldsymbol{x}_t$ was expressed as an interpolated version of the climatological profiles discretized densely close to the observer and coarsely far from the observer. In this case, the temperature profile as a function of altitude was the only target parameter to be retrieved and the state vector $\boldsymbol{x}$ consisted of 19 data points per profile.

Table 1 lists the values of the nonlinearity parameter computed by Eq. (5). Here, 8 out of 10 values are less than one, indicating that within the assumed range of variation of the a priori state, the effect of the nonlinearity is mostly less than that of the measurement error. Accordingly, this problem does not appear to be severely nonlinear.

3.1. Performance of direct regularization

In the first numerical experiment, we analyze the performance of the five regularization parameter selection methods. For each $\boldsymbol{y}_i^\delta$, λ_i was estimated by a specific parameter selection method. Calculations by repeating the

Please cite this article as: Xu J, et al. Assessment of Tikhonov-type regularization methods for solving atmospheric inverse problems. J Quant Spectrosc Radiat Transfer (2016), http://dx.doi.org/10.1016/j.jqsrt.2016.08.003

inversions for all realizations of the noisy data were performed. The retrievals were done with the same setting: the initial guess $\boldsymbol{x}_0$ was chosen as a height-constant profile and the a priori profile $\boldsymbol{x}_a$ was taken as AFGL's U.S. standard atmosphere (i.e. G06). Too small λ produces undersmoothness which entails more oscillatory artefacts around the exact profile, whereas too large λ produces oversmoothness which shows less oscillations and a similar shape to that of the a priori profile.

Fig. 2 displays the difference per altitude level between the retrieved profiles and the exact profiles for the five regularization parameter selection methods and the noise standard deviation $\sigma = 0.1$. The inversion accuracy for all methods turns out to be much higher when the exact

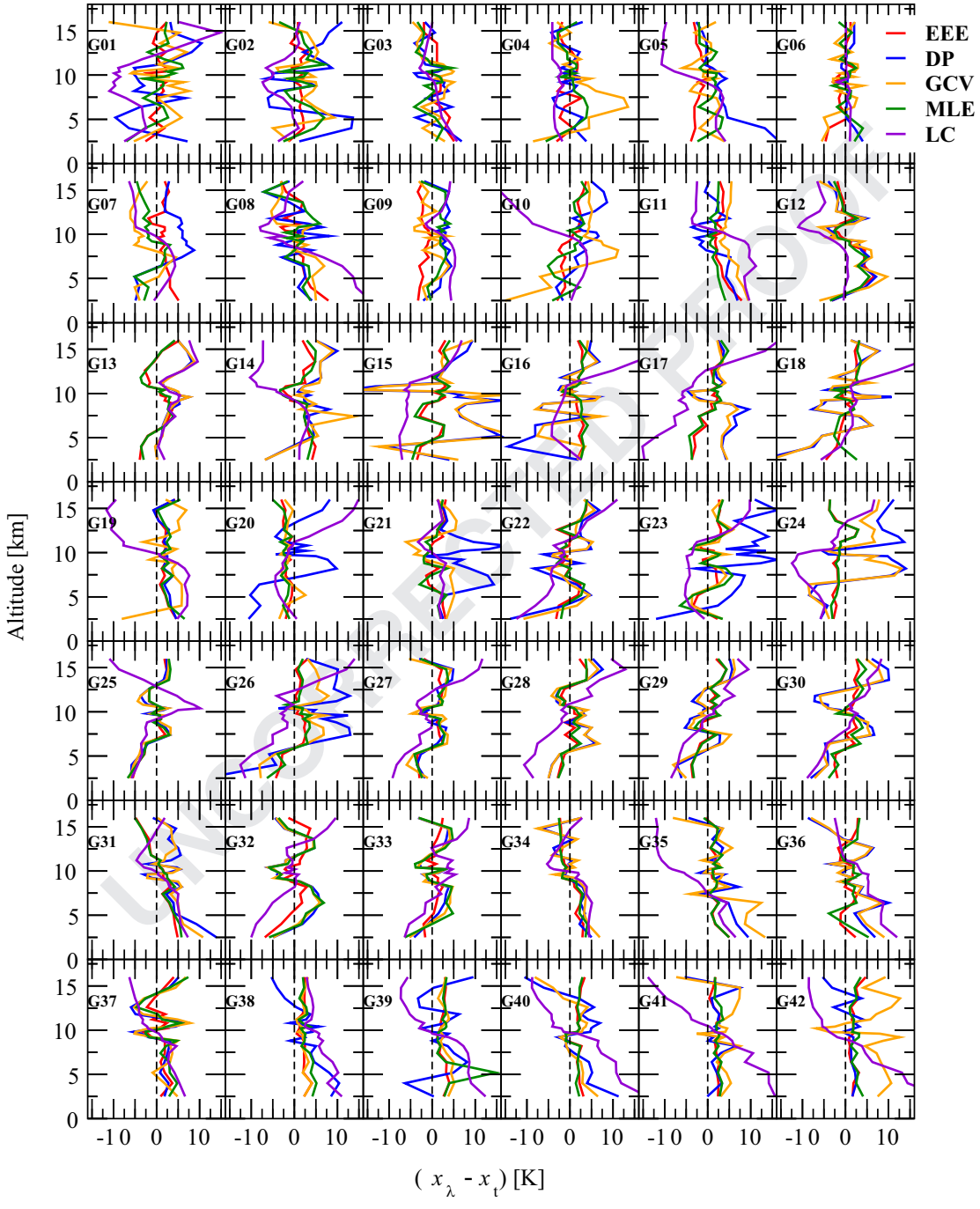

Fig. 2. Comparison of retrieved temperature profiles with exact profiles as a function of altitude for five regularization parameter selection methods. Results of 42 atmospheres for the noise standard deviation $\sigma = 0.1$ are presented. The plotted altitude range of 2.5–16 km is the altitude range which can be observed by MTP with confidence. The retrieval beyond this altitude range has little physical meaning.

Please cite this article as: Xu J, et al. Assessment of Tikhonov-type regularization methods for solving atmospheric inverse problems. J Quant Spectrosc Radiat Transfer (2016), http://dx.doi.org/10.1016/j.jqsrt.2016.08.003

profile has an identical or similar shape to the a priori profile, e.g. for the G06 and G34 atmospheres. The value of λ chosen by DP and GCV is obviously too small so that the differences are larger, e.g. for the G15 and G16 atmospheres. In the case of the G12 and G18 atmospheres, the exact profile at lower altitudes is very similar to the a priori one but the discrepancies increase when the altitude increases. It can be deduced from both retrievals that λ estimated by LC is too large so that the differences between the retrieved profiles and the exact profiles become larger at higher altitudes.

All retrieved profiles using λ chosen by the EEE method resemble the shape of the exact profile and the magnitude of the solution only differ slightly from that of the exact profile. The MLE method produces, indubitably, the second highest inversion accuracy and the estimated λ only occasionally leads to undersmoothed solutions. Given the fact that the retrieved profiles corresponding to DP and GCV show frequently an undersmoothed behavior, we may conclude that λ chosen by these two methods imposes originally a too weak regularization. Surprisingly, the LC method does not perform as good as expected, and to some extent, the estimated λ leads to strong regularization as compared to that by other methods. The results reveal that the retrieved profiles are a bit oversmoothed and tend towards the a priori.

The average absolute differences over 42 atmospheres corresponding to various regularization parameter selection strategies for all three noise scenarios are plotted in Fig. 3. When the measurement is noisier, the deviation from the exact profile is larger. This tendency is more recognizable in the case of GCV and less recognizable in the case of LC. However, both EEE and MLE work stably and always attain the best two results. In most cases, it is more challenging to seek a reasonable retrieval at altitudes where the sensitivity of the instrument is low. As a result, the difference is smaller around 10 km and is larger when the grid point is far from the instrument. In addition, these average differences are consistent with the median value for each altitude level.

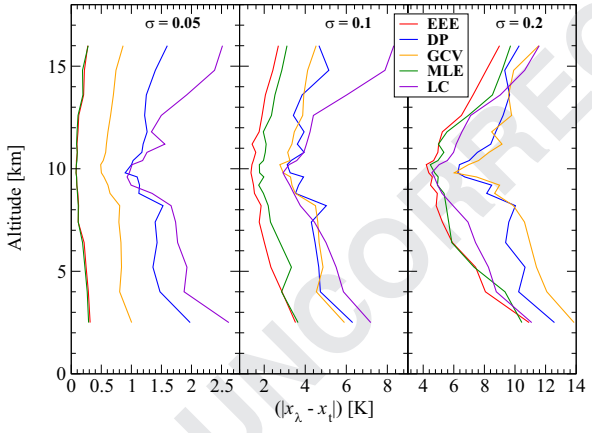

Fig. 3. Average absolute difference as a function of altitude over 42 atmospheres for five regularization parameter selection methods.

More diagnostic quantities reflect the retrieval performance of different regularization parameter selection methods, as inferred from Figs. 2 and 3. The average values of the solution errors and residual over noisy data realizations and for all noise standard deviations (σ) are presented in Table 2, regardless of whether the particular method fails in some situations. In this work, the solution error is calculated as the root mean square error (RMSE) and the residual is given in terms of residual sum of squares. The average values of the DOFS related to the smoothing error and giving information about the useful independent quantities in the measurement are also given for the three noise standard deviations.

Most regularization parameter selection strategies result in comparable residuals after convergence for the three noise realizations. Both EEE and MLE outclass the other methods in terms of the inversion accuracy. The smallest solution errors are obtained by EEE except for the scenario $\sigma = 0.05$. By comparing the corresponding residuals and DOFS, all methods convergence with similar performance and the LC method yields slightly worse results. In the case of $\sigma = 0.2$, small discrepancies in the DOFS reveal that all methods make use of comparable information content from the measurement. The same holds true for the vertical resolution: LC results in a worse vertical resolution than the other methods, especially for data with small noise levels.

In these three noise standard deviation scenarios, the retrieval performance of EEE is generally better than those of the other methods, although the minimization of the expected error using a random solution domain is a bit cost prohibitive. Furthermore, λ does not vary significantly for different $\boldsymbol{y}^{\delta}$ and the same σ. The reason is that the a priori parameter selection rule is only dependent on the noise level. In principle, the expected error given in Eq. (7) also incorporates model parameters errors and we are

Table 2
Average values of solution errors (RMSE, in units of K) and residuals (residual sum of squares, in units of K^2) of temperature retrieval for different regularization parameter selection methods. For each retrieval case, λ was estimated by EEE, DP, GCV, MLE, and LC, respectively. In addition, average values of the DOFS are listed.

Method	Solution error			Residual			DOFS		
	$\sigma = 0.05$	$\sigma = 0.1$	$\sigma = 0.2$	$\sigma = 0.05$	$\sigma = 0.1$	$\sigma = 0.2$	$\sigma = 0.05$	$\sigma = 0.1$	$\sigma = 0.2$
EEE	0.15	2.18	6.36	3.01	12.51	21.49	15.82	13.58	11.46
DP	1.31	4.84	9.02	3.97	13.74	20.70	15.07	12.91	12.27
GCV	0.70	4.47	9.73	3.15	13.38	20.28	15.33	13.14	12.08
MLE	0.12	2.69	6.79	3.04	11.21	22.12	15.71	14.27	10.95
LC	1.68	5.77	7.45	4.95	16.06	22.75	13.54	10.70	9.88

Please cite this article as: Xu J, et al. Assessment of Tikhonov-type regularization methods for solving atmospheric inverse problems. J Quant Spectrosc Radiat Transfer (2016), http://dx.doi.org/10.1016/j.jqsrt.2016.08.003

aware that uncertainties in atmospheric profiles, molecular spectroscopy, and instrument parameters cause additional errors in the retrieval. In spite of that, an extended discussion of potential error sources beyond the smoothing and noise errors is not considered in this temperature retrieval problem.

Concerning the DP method, the control parameter χ may always be chosen from sufficiently large, giving a solvable discrepancy principle equation. However, in fact, the iteration in many cases stops too early with a non-satisfying result. In contrast, a sufficient decrease of χ may let the iteration stop too late with a bad result because it returns a too small λ corresponding to a too weak regularization, and consequently, the retrieval sometimes achieves an undersmoothed solution, albeit giving a very small residual. As shown in Table 3, the value $\chi = 1.05$ yields the smallest solution error for the first six atmospheric configurations (i.e. AFGL profiles) and has been adopted in our analysis.

Likewise, the GCV method sometimes fails to locate an optimal λ because of an extremely flat minimum in the curve, i.e. a number of additional local minima of $V(\lambda)$ in Eq. (14) are found over a wide range of parameters λ. This makes it difficult to search for the optimal λ numerically. In this dilemma, a too small λ may be selected, yielding a weaker regularization.

In most of the cases, MLE delivers solution errors as small as EEE, only occasionally it predicts a too small λ, producing an underregularized solution. From a theoretical point of view, the ML function and the GCV function both use the term $(\mathbf{I}_m - \mathbf{K}\mathbf{K}_\lambda^\dagger)$ and are supposed to behave in an analogous manner.

The LC method would have been expected to give a good prediction of λ stemming from its robustness (also known from a number of applications in atmospheric remote sensing, e.g. [39–41]). However, values of λ for all three noise realizations are slightly overestimated and produce oversmoothed solutions and larger residuals. Hansen [42] observed that this method tends to produce overregularization in some specific inverse problems. LC is also characterized by a saturation effect, which means that the solution error does not significantly decrease with decreasing σ as the other methods do. For a larger σ, LC obtains an improved retrieval performance (see also Fig. 3 and Table 2).

Error-free parameter selection methods seem more tempting, as these methods do not rely on information about the data error, which is particularly convenient for resolving real practical problems. In Fig. 4, a selection process of λ using GCV, MLE, and LC is exemplified by the temperature retrieval from a noisy data. The pattern of the ML function (16) is similar to that of the GCV function (14), but the minimum is not that flat. In many cases, a sharper minimum in the curve of the ML function makes it easier to find the regularization parameter using MLE. Regarding the LC method, the characteristic "L"-shape is slightly lost when σ is higher.

The solution errors listed in Table 4 indicate that MLE predicts the best choice of λ among these three methods. GCV could lead to an underestimation of λ due to a flat minimum in the function curve, while LC may give an overestimation of λ due to a curve with an indistinct corner. Due to the dependency of the DOFS on the regularization strength, a solution with the highest and lowest values of the DOFS corresponds to GCV and LC, respectively.

Table 3
Average values of solution errors [K] corresponding to the DP method. The temperature retrievals corresponding to the six AFGL atmospheres were done with λ estimated by DP for different values of χ.

χ	Solution error		
	$\sigma = 0.05$	$\sigma = 0.1$	$\sigma = 0.2$
1.01	2.01	5.41	10.03
1.03	1.87	5.12	9.85
1.05	1.51	4.86	9.11
1.10	1.76	5.35	10.23
1.50	2.47	7.00	12.34
2.00	3.14	7.73	13.90
2.50	3.89	8.99	15.05

Based on the results above, the regularization parameter selection methods can be sorted based on their performance:

Good: EEE and MLE;
Fair: LC;
Poor: DP and GCV.

It is plain to see that the regularization parameter λ predicted by EEE and MLE often stabilizes the inversion procedure via a suitable strength which produces a retrieval with small solution error, good fit to the data, and adequate use of information from the measurement. Although LC sometimes leads to oversmoothing and the retrieval is accordingly affected by the a priori knowledge, we rank this method ahead of DP and GCV due to its consistency and stability. DP and GCV turn out to be inferior to the other parameter selection methods, as both methods have a certain deficiency in characterizing the smoothness of the solution. However, it would be problematic to reach any general conclusions from this application, since the quality of the fit is profoundly governed by the physical properties of the specific measurement condition.

3.2. Performance of iterative regularization

Iterative regularization methods employ some rules for stopping the iteration suitably and do not require an elaborate computation for λ, which can greatly reduce the running time of a complete inversion process. Here, the temperature retrievals using the IRGN method were carried out. An important issue of any iterative method is the value of the control parameter χ when using the discrepancy principle as the stopping criterion (Eq. (20)). The optimal choice of χ is dependent on the specific problem to be solved.

The second parameter that affects the retrieval is the ratio r of the λ-sequence in Eq. (19). In Fig. 5, the solution errors and the corresponding number of iterations for different values of r are plotted. The experiments were carried out for the six AFGL atmospheric configurations.

Please cite this article as: Xu J, et al. Assessment of Tikhonov-type regularization methods for solving atmospheric inverse problems. J Quant Spectrosc Radiat Transfer (2016), http://dx.doi.org/10.1016/j.jqsrt.2016.08.003

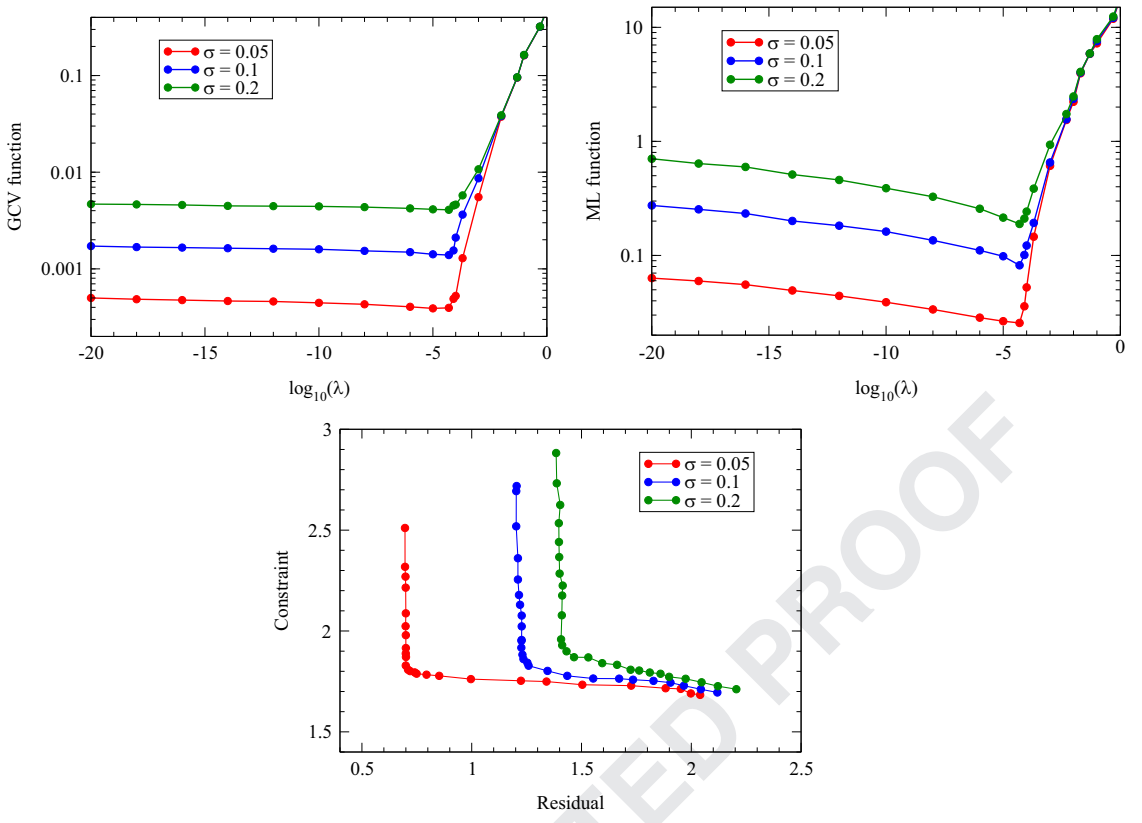

Fig. 4. Selection of λ using GCV, MLE, and LC corresponding to different values of the noise standard deviation σ. The curves are plotted for a temperature retrieval problem.

Table 4
Regularization parameter λ and solution errors [K] corresponding to the following error-free selection methods: GCV, MLE, and LC.

Method	λ			Solution error		
	$\sigma = 0.05$	$\sigma = 0.1$	$\sigma = 0.2$	$\sigma = 0.05$	$\sigma = 0.1$	$\sigma = 0.2$
GCV	1.55×10^{-5}	1.96×10^{-5}	2.70×10^{-5}	0.69	4.39	8.85
MLE	4.13×10^{-5}	5.34×10^{-5}	6.05×10^{-5}	0.17	2.45	6.60
LC	7.97×10^{-5}	8.80×10^{-5}	1.46×10^{-4}	0.54	5.39	7.02

Apparently, the retrieval using a larger value of r requires a larger number of iteration steps as can be seen from the right panel of Fig. 5. A value approaching 1 indicates that λ is supposed to gradually decrease during the iteration and is advisable to obtain better approximations of the exact profile.

For each σ, we repeated the retrievals over 42 noisy data realizations by using IRGN. A comparison of the solution errors of every single retrieval corresponding to IRGN and TR is illustrated in Fig. 6. In this case, the results of TR are plotted for the EEE method (referred to TR-EEE in the figure) which provides the best estimates in Section 3.1. It can be seen that both regularization schemes show similar performance and the average values of the solution errors over the three noise scenarios are nearly equivalent. In this regard, we can conclude that both regularization schemes obtain almost the same inversion accuracy.

In addition to the inversion accuracy, IRGN is superior to TR because of its efficiency in estimating the regularization parameter. In the next section, we perform trace gas retrievals from the actual TELIS data in order to further compare these two regularization algorithms.

4. Trace gas retrieval

In this section, trace gas profiles retrieved from real TELIS measurements are presented. Here, $\boldsymbol{y}^{\delta}$ represents a limb sequence of far infrared radiance spectra (in units of $[\mathrm{W}/(\mathrm{m}^2\,\mathrm{sr}\,\mathrm{Hz})]$) recorded by the 1.8 THz channel. Fig. 7 illustrates a sequence of radiance spectra in the CO microwindow from the second Kiruna flight which took place on 24 January 2010. The flight altitude was about 33.5 km. A microwindow contains four spectral segments (500 MHz for each). The discontinuities between adjacent spectral

Please cite this article as: Xu J, et al. Assessment of Tikhonov-type regularization methods for solving atmospheric inverse problems. J Quant Spectrosc Radiat Transfer (2016), http://dx.doi.org/10.1016/j.jqsrt.2016.08.003

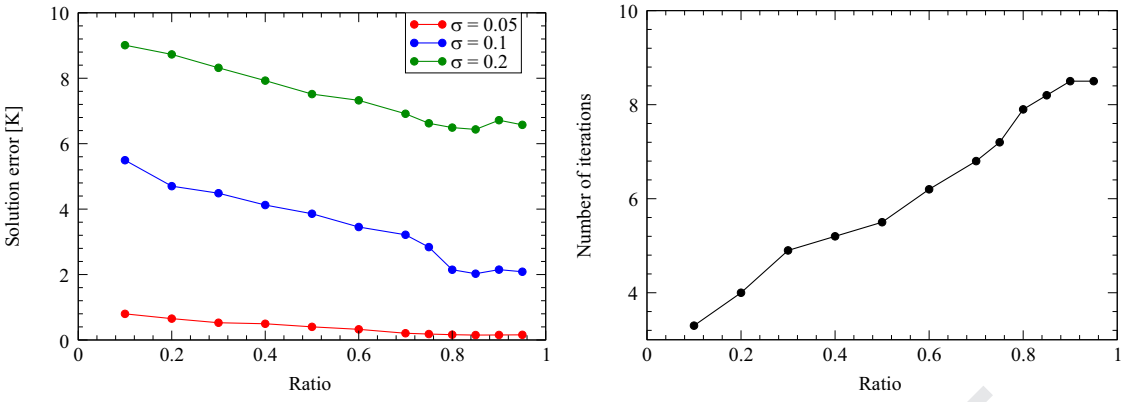

Fig. 5. Average values of solution errors and number of iterations for the IRGN method. The retrievals were done for the six AFGL atmospheres with different values of r.

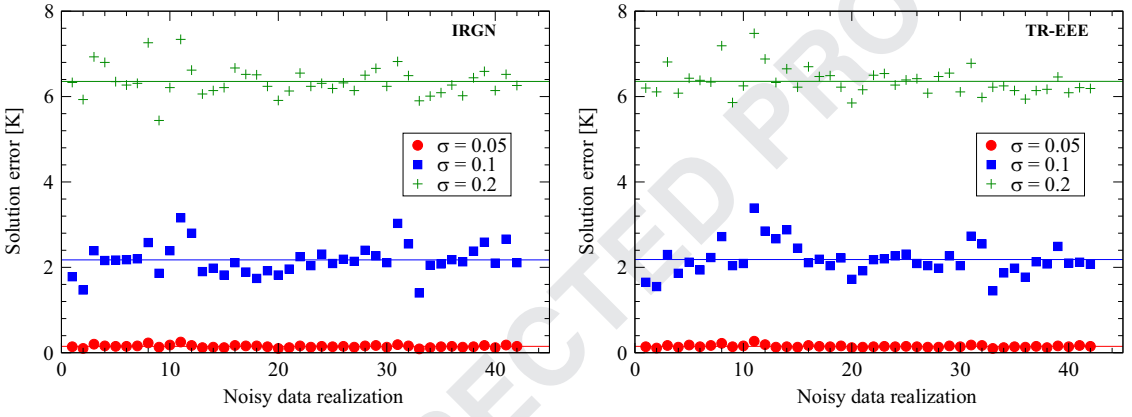

Fig. 6. Solution errors for IRGN (left) and TR with the EEE method (right). The results correspond to $\sigma = 0.05$ (circle), $\sigma = 0.1$ (square), and $\sigma = 0.2$ (plus). The horizontal lines refer to the average values of the solution errors.

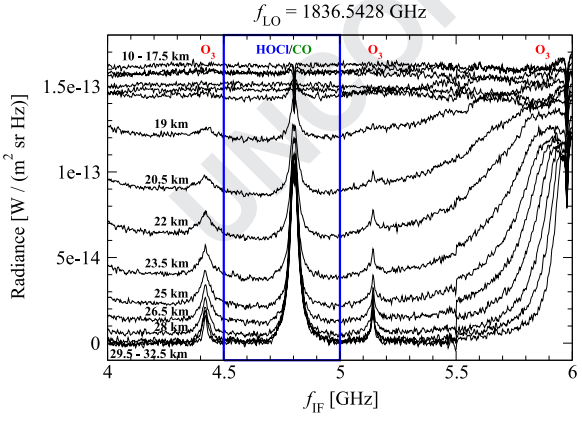

Fig. 7. A sequence of limb spectra in the CO microwindow measured by the TELIS 1.8 THz channel during the 2010 flight. The limb sequence observing a CO line and covering tangent heights between 10 and 32.5 km in steps of 1.5 km is illustrated as a function of the intermediate frequency f_{IF}. The spectral segment of 500 MHz selected for CO retrieval is indicated by a blue rectangular box. The dedicated measurement identifier is 20,864. (For interpretation of the references to color in this figure caption, the reader is referred to the web version of this paper.)

segments are most likely produced by baseline shifts and variations in the spectral response across the segments.

It can be noticed that the O_3 and CO transitions are identifiable and isolated from each other, thus, we retrieved O_3 and CO individually from the first segment and the second segment, respectively. In this way, the baseline fitting could be improved and the effects from other interfering molecular features can be reduced. In addition to the target molecule, we retrieved a so-called "graybody" for compensating "continuum-like contributions" and a polynomial for instrument baseline offset.

The TELIS profiles were retrieved with direct and iterative regularization methods. Table 5 lists the chosen λ corresponding to the two regularization algorithms. In the case of TR, the EEE and MLE methods were used and the resulting values of λ were essentially equivalent (we do not distinguish between EEE and MLE hereafter in this section), while for IRGN, the control parameter $\chi = 1.02$ was used for this problem. An overall accuracy for the most possible error sources (smoothing, noise, and model parameters) was estimated for each retrieval.

Please cite this article as: Xu J, et al. Assessment of Tikhonov-type regularization methods for solving atmospheric inverse problems. J Quant Spectrosc Radiat Transfer (2016), http://dx.doi.org/10.1016/j.jqsrt.2016.08.003

For comparison, the retrieved concentration profiles obtained by two spaceborne limb sounders JEM/SMILES (Japanese Experiment Module/Superconducting subMIllimeter-wave Limb-Emission Sounder) [43] and Aura/MLS (Microwave Limb Sounder) [44] were considered. The SMILES profiles were taken from the NICT (National Institute of Information and Technology) Level-2 research product (available at http://smiles.nict.go.jp/pub/data/) and the MLS profiles were provided by JPL (available at https://mls.jpl.nasa.gov/index-eos-mls.php). The retrieval algorithms for both instruments [45,46] implement the optimal estimation method (OEM) [16] based on Bayes' theorem.

A comparison of ozone retrieval between TELIS, SMILES, and MLS profiles is shown in the left panel of Fig. 8. Two SMILES profiles and one MLS profile which were geographically and temporally coincident with the TELIS profiles are plotted. These three independent profiles fall well within the error margin of the TELIS profiles (see dashed lines in Fig. 8) and an encouraging agreement is reached between 13 and 35 km. The two TELIS profiles obtain virtually identical shape, and the magnitude of the O_3 profile estimated by TR is slightly higher above 20 km. In the right panel of Fig. 8, two CO retrievals using TR and IRGN, respectively, are compared against the MLS retrieval. Evidently, the MLS profile mostly falls within the accuracy domain of the two TELIS profiles. The two regularization schemes result in retrievals with large error budget below 15 km and above 32 km due to regularization. Both TELIS profiles have virtually identical shape and capture the peak at 32.5 km, which is consistent with the MLS profile.

Table 6 summarizes the number of iterations and the residuals for the direct and iterative regularization methods. In the case of IRGN, the convergence took a few more iteration steps, but the residual sum of squares after convergence turned out to be a bit smaller. Furthermore, the additional computation time for choosing λ (typically longer than 2 h) in the method of TR has to be taken into account, whereas the initial λ for the IRGN method can be chosen relatively easily. The differences in the DOFS between these two methods prove that IRGN extracts more useful information from the measurement. A better vertical resolution of IRGN ($\sim$1.7–3 km) also shows signs of improvement over TR ($\sim$1.9–3.3 km).

For trace gas retrievals, an overall agreement between the two TELIS profiles ensures the consistency of retrieval solutions using the two regularization methods. The quality of both TELIS profiles is in line with the profiles derived from SMILES and MLS. The discrepancies between different instruments at lower altitudes are subject to different a priori information.

Consequently, this application on real measurements suggests that there are no fundamental differences between IRGN and TR in the final profiles. Instead, our focus can be put on the simplicity and effort required to produce best possible inversion accuracy with the two methods. Although TR is faster than IRGN to reach convergence, this improvement is the price that we have to pay for good estimates of the true state over a wide range of values of λ. As an overestimated λ does not affect the final solution, IRGN can substantially save the effort for

Table 5
Regularization parameters used for TELIS retrievals. For IRGN, λ represents the initial regularization parameter. Additionally, the ratio r of the λ-sequence is given in parentheses.

Method	O_3	CO
TR	0.75	1.70×10^{-3}
IRGN	20.00 (0.85)	0.10 (0.85)

Table 6
Number of iterations, residual, and DOFS after convergence for TR and IRGN.

Problem	Method	Number of iterations	Residual	DOFS
O_3	TR	12	3.795	7.44
	IRGN	14	3.286	12.23
CO	TR	10	12.903	10.46
	IRGN	13	11.372	13.51

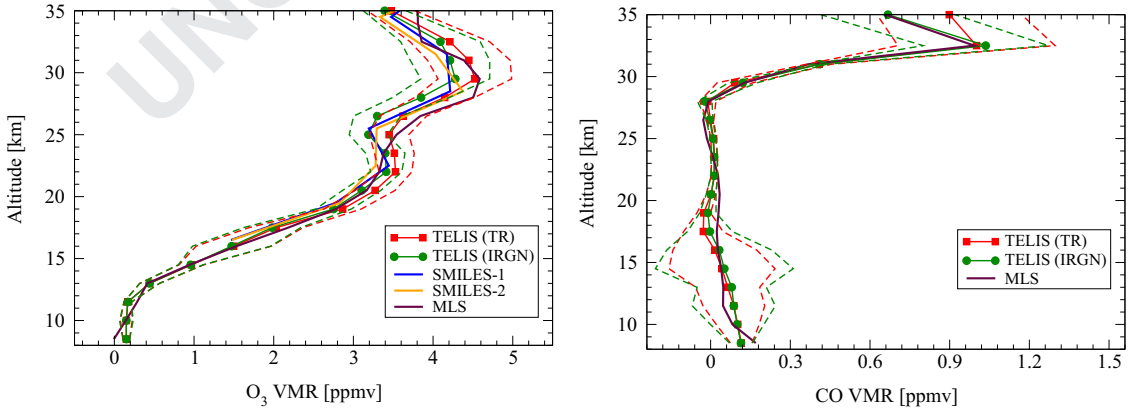

Fig. 8. Comparison of O_3 and CO concentration profiles retrieved from TELIS, SMILES, and MLS data measured on 24 January 2010. Two TELIS profiles were retrieved using TR and IRGN, respectively. The lowest tangent height of TELIS is 10 km and the retrieval results below this altitude have little physical meaning. The dashed lines refer to the overall accuracy of the two TELIS profiles. The time difference of all plotted measurements was within 0.5 h. The MLS profile was linearly interpolated onto the retrieval grid of the TELIS retrieval by taking the averaging kernel into account.

Please cite this article as: Xu J, et al. Assessment of Tikhonov-type regularization methods for solving atmospheric inverse problems. J Quant Spectrosc Radiat Transfer (2016), http://dx.doi.org/10.1016/j.jqsrt.2016.08.003

estimating a proper λ. Additionally, IRGN achieves a marginally better fit to the data (smaller residual) and an enhanced use of information from the measurement itself (higher DOFS).

5. Conclusions

We have presented several Tikhonov-type regularization schemes for solving atmospheric inverse problems and investigated the numerical performance by retrieving vertical distributions of temperature and trace gas profiles from microwave and far infrared observations.

The objective of this study has been an assessment of several well-established regularization parameter selection methods that critically impact the performance of an inversion algorithm. On the subject of direct TR, the regularization parameter λ has to be chosen through an optimal compromise between stability and accuracy. Various strategies for selecting the regularization parameter have been briefly described, including EEE (using a priori selection rule); DP (using a posteriori selection rule); and GCV, MLE, and LC (using error-free selection rule). Their pros and cons have been studied by retrieving temperature profiles from synthetic MTP data. The retrieval quality has been quantitatively analyzed through the solution error, residual, and DOFS.

From our numerical analysis we may draw the following conclusions:

- The value of λ predicted by the EEE method often gives the best estimate of the retrieval solution, but this method, by its nature, demands the knowledge of a solution domain with physical meaning.
- An inherent weakness in the DP method may be that the solution errors are very sensitive to the control parameter χ. This observation has been made in numerical tests: χ should be chosen neither too small nor too large.
- The GCV curve may possess a peculiarly flat minimum, making it difficult to locate the optimal λ.
- The numerical performance of the MLE method is on a par with that of EEE, but occasional failures of λ generate underregularized solutions.
- The LC method sometimes leads to unconvincing retrieval performance with overestimated λ, even though it is very efficient for data with large noise levels.

Practical implementations of different parameter selection methods demonstrate that at the present stage, there is no method balancing up accuracy and efficiency in the best possible manner. Each method has its own deficiencies in either computational complexity or retrieval reliability. Nevertheless, error-free parameter selection methods would be more attractive in the analysis of real measurements, due to the challenges associated with estimating the data error in practice.

These discoveries raise an intriguing question: Is there any useful way to somewhat spare computational effort of obtaining an ideal λ? IRGN, as a typical iterative regularization method, simplifies the estimation of λ and appears to offer retrieval results as good as TR. This method is favorable because it is insensitive to overestimations of λ. Whereas λ characterizes the regularization strength in the framework of direct regularization methods, the number of iterations acts as a regularization parameter in the framework of iterative regularization methods where the discrepancy principle is used as a stopping criterion. The conducted temperature retrievals point out the importance of the control parameter χ in the stopping rule and the ratio r of the λ-sequence.

Whether iterative regularization methods manage to produce promising approximations of the solution compared to direct regularization methods, has also been assessed by trace gas retrievals from real TELIS limb spectra. The profile computed by the IRGN method closely approaches the one computed by the means of TR and other spaceborne data products, by consuming only a few more iteration steps. The results also show that IRGN surpasses TR regarding the goodness of fit (residual) and the exploitation of information from the measurement (DOFS).

Iterative regularization methods may not be an impeccable choice all the time, giving the reason that a robust stopping rule and the characterization of the λ-sequence need some further investigations. Nevertheless, our findings indicate that IRGN is a reliable alternative to TR for solving ill-posed inverse problems.

Acknowledgments

The authors would like to thank M. Birk, G. Wagner, and P. Vogt from DLR for processing the TELIS Level-1 calibrated data. Special thanks would go to M. Kenntner and M. Rapp for many fruitful discussions on the MTP retrieval configurations. The authors would gratefully acknowledge the Level-2 data processing team from NICT and JPL for sharing the retrieved atmospheric profiles obtained by SMILES and MLS.

References

[1] Tikhonov AN. On the solution of incorrectly stated problems and a method of regularization. Dokl Acad Nauk SSSR 1963;151:501–4.
[2] Engl HW, Hanke M, Neubauer A. Regularization of inverse problems. Dordrecht, The Netherlands: Kluwer Academic Publishers; 2000.
[3] Vogel CR. Computational methods for inverse problems. Philadelphia, PA: SIAM; 2002.
[4] Doicu A, Trautmann T, Schreier F. Numerical regularization for atmospheric inverse problems. Berlin, Heidelberg, Germany: Springer-Verlag; http://dx.doi.org/10.1007/978-3-642-05439-6.
[5] Wu L. A parameter choice method for Tikhonov regularization. Electron Trans Numer Anal 2003;16:107–28.
[6] Ceccherini S. Analytical determination of the regularization parameter in the retrieval of atmospheric vertical profiles. Opt Lett 2005;30(19):2554–6. http://dx.doi.org/10.1364/OL.30.002554.
[7] Ridolfi M, Sgheri L. Iterative approach to self-adapting and altitude-dependent regularization for atmospheric profile retrievals. Opt Express 2011;19(27):26696–709. http://dx.doi.org/10.1364/OE.19.026696.
[8] Naeimi M, Flury J, Brieden P. On the regularization of regional gravity field solutions in spherical radial base functions. Geophys J Int 2015;202(2):1041–53. http://dx.doi.org/10.1093/gji/ggv210.
[9] Albani V, De Cezaro A, Zubelli JP. On the choice of the Tikhonov regularization parameter and the discretization level: a

discrepancy-based strategy. Inverse Probl Imaging 2016;10(1):1–25. http://dx.doi.org/10.3934/ipi.2016.10.1.

[10] Steck T. Methods for determining regularization for atmospheric retrieval problems. Appl Opt 2002;41(9):1788–97. http://dx.doi.org/10.1364/AO.41.001788.

[11] Farquharson CG, Oldenburg DW. A comparison of automatic techniques for estimating the regularization parameter in non-linear inverse problems. Geophys J Int 2004;156(3):411–25. http://dx.doi.org/10.1111/j.1365-246X.2004.02190.x.

[12] Denning RF, Guidero SL, Parks GS, Gary BL. Instrument description of the airborne microwave temperature profiler. J Geophys Res 1989;94:16757–65. http://dx.doi.org/10.1029/JD094iD14p16757.

[13] Mahoney MJ, Denning R. A state-of-the-art airborne microwave temperature profiler (MTP). In: Proceedings of the 33rd international symposium on the remote sensing of the environment, Stresa, Italy; May 2009.

[14] Birk M, Wagner G, de Lange G, de Lange A, Ellison BN, Harman MR, et al. TELIS: TErahertz and subMMW LImb Sounder – project summary after first successful flight. In: Proceedings of 21st international symposium on space terahertz technology. University of Oxford and STFC Rutherford Appleton Laboratory; 2010. p. 195–200.

[15] Friedl-Vallon F, Maucher G, Seefeldner M, Trieschmann O, Kleinert A, Lengel A, et al. Design and characterization of the balloon-borne Michelson interferometer for passive atmospheric sounding (MIPAS-B2). Appl Opt 2004;43(16):3335–55. http://dx.doi.org/10.1364/AO.43.003335.

[16] Rodgers CD. Inverse methods for atmospheric sounding: theory and practise. Singapore: World Scientific; 2000.

[17] Morozov VA. On the solution of functional equations by the method of regularization. Sov Math Dokl 1966;7:414–7.

[18] Wahba G. Practical approximate solutions to linear operator equations when the data are noisy. SIAM J Numer Anal 1977;14:651–67.

[19] Wahba G. Spline models for observational data. Philadelphia, PA: SIAM; 1990.

[20] Demoment G. Image reconstruction and restoration: overview of common estimation structures and problems. IEEE Trans Acoust Speech Signal Process 1989;37(12):2024–36. http://dx.doi.org/10.1109/29.45551.

[21] Hansen PC. Analysis of discrete ill-posed problems by means of the L-curve. SIAM Rev 1992;34:561–80. http://dx.doi.org/10.1137/1034115.

[22] Eriksson J. Optimization and regularization of nonlinear least squares problems [Ph.D. thesis]. Umeå, Sweden: Department of Computing Science, Umeå University; 1996.

[23] Eriksson P. Analysis and comparison of two linear regularization methods for passive atmospheric observation. J Geophys Res 2000;105(D14):18157–67. http://dx.doi.org/10.1029/2000JD900172.

[24] Hansen PC, O'Leary DP. The use of the L-curve in the regularization of discrete ill-posed problems. SIAM J Sci Comput 1993;14:1487–503.

[25] Bakushinskii AB. The problem of the convergence of the iteratively regularized Gauss–Newton method. Comput Math Math Phys 1992;32(9):
1353–9 URL ⟨http://dl.acm.org/citation.cfm?id=157916.157930⟩.

[26] Doicu A, Schreier F, Hess M. Iteratively regularized Gauss–Newton method for atmospheric remote sensing. Comput Phys Commun 2002;148:214–26. http://dx.doi.org/10.1016/S0010-4655(02)00555-6.

[27] Doicu A, Schreier F, Hess M. Iteratively regularized Gauss–Newton method for bound-constraint problems in atmospheric remote sensing. Comput Phys Commun 2003;153(1):59–65. http://dx.doi.org/10.1016/S0010-4655(03)00138-3.

[28] Xu J, Schreier F, Vogt P, Doicu A, Trautmann T. A sensitivity study for far infrared balloon-borne limb emission sounding of stratospheric trace gases. Geosci Instrum Methods Data Syst Discuss 2013;3(1):251–303. http://dx.doi.org/10.5194/gid-3-251-2013.

[29] Kaltenbacher B, Neubauer A, Scherzer O. Iterative regularization methods for nonlinear problems. Berlin, New York: de Gruyter; 2008.

[30] Schreier F, Gimeno García S, Hedelt P, Hess M, Mendrok J, Vasquez M, et al. GARLIC—a general purpose atmospheric radiative transfer line-by-line infrared-microwave code: implementation and evaluation. J Quant Spectrosc Radiat Transf 2014;137:29–50. http://dx.doi.org/10.1016/j.jqsrt.2013.11.018.

[31] Gimeno García S, Schreier F, Lichtenberg G, Slijkhuis S. Near infrared nadir retrieval of vertical column densities: methodology and application to SCIAMACHY. Atmos Meas Tech 2011;4(12):2633–57. http://dx.doi.org/10.5194/amt-4-2633-2011.

[32] Griewank A. Evaluating derivatives: principles and techniques of algorithmic differentiation. Philadelphia, PA: SIAM; 2000.

[33] Naumann U. The art of differentiating computer programs: an introduction to algorithmic differentiation. Philadelphia, PA: SIAM; http://dx.doi.org/10.1137/1.9781611972078.

[34] Schreier F, Gimeno García S, Vasquez M, Xu J. Algorithmic vs. finite difference Jacobians for infrared atmospheric radiative transfer. J Quant Spectrosc Radiat Transf 2015;164:147–60. http://dx.doi.org/10.1016/j.jqsrt.2015.06.002.

[35] Hascoët L, Pascual V. The Tapenade automatic differentiation tool: principles, model, and specification. ACM Trans Math Softw 2013;39(3). http://dx.doi.org/10.1145/2450153.2450158.

[36] Garand L, Turner DS, Larocque M, Bates J, Boukabara S, Brunel P, et al. Radiance and Jacobian intercomparison of radiative transfer models applied to HIRS and AMSU channels. J Geophys Res 2001;106(D20):24017–31. http://dx.doi.org/10.1029/2000JD000184.

[37] Anderson GP, Clough SA, Kneizys FX, Chetwynd JH, Shettle EP. AFGL atmospheric constituent profiles (0–120 km). Technical report TR-86-0110, AFGL; 1986.

[38] Turner DS. Absorption coefficient estimation using a two-dimensional interpolation procedure. J Quant Spectrosc Radiat Transf 1995;53:633–7. http://dx.doi.org/10.1016/0022-4073(95)00024-F.

[39] de Lange A, Birk M, de Lange G, Friedl-Vallon F, Kiselev O, Koshelets V, et al. HCl and ClO in activated Arctic air; first retrieved vertical profiles from TELIS submillimetre limb spectra. Atmos Meas Tech 2012;5(2):487–500. http://dx.doi.org/10.5194/amt-5-487-2012.

[40] Schepers D, Guerlet S, Butz A, Landgraf J, Frankenberg C, Hasekamp O, et al. Methane retrievals from Greenhouse Gases Observing Satellite (GOSAT) shortwave infrared measurements: performance comparison of proxy and physics retrieval algorithms. J Geophys Res 2012;117(D10):D10307. http://dx.doi.org/10.1029/2012JD017549.

[41] Borsdorff T, Hasekamp OP, Wassmann A, Landgraf J. Insights into Tikhonov regularization: application to trace gas column retrieval and the efficient calculation of total column averaging kernels. Atmos Meas Tech 2014;7(2):523–35. http://dx.doi.org/10.5194/amt-7-523-2014.

[42] Hansen PC. The L-curve and its use in the numerical treatment of inverse problem. In: Johnston PR, editor. Computational inverse problems in electrocardiology, Advances in computational bioengineering, vol. 5. Southampton: WIT Press; 2001. p. 119–42.

[43] Kikuchi K, Nishibori T, Ochiai S, Ozeki H, Irimajiri Y, Kasai Y, et al. Overview and early results of the Superconducting Submillimeter-Wave Limb-Emission Sounder (SMILES). J Geophys Res 2010;115(D23):D23306. http://dx.doi.org/10.1029/2010JD014379.

[44] Waters JW, Froidevaux L, Harwood RS, Jarnot RF, Pickett HM, Read WG, et al. The earth observing system microwave limb sounder (EOS MLS) on the Aura satellite. IEEE Trans Geosci Remote Sens 2006;44(5):1075–92. http://dx.doi.org/10.1109/TGRS.2006.873771.

[45] Livesey NJ, VanSnyder W, Read WG, Wagner PA. Retrieval algorithms for the EOS Microwave Limb Sounder (MLS). IEEE Trans Geosci Remote Sens 2006;44(5):1144–55. http://dx.doi.org/10.1109/TGRS.2006.872327.

[46] Baron P, Urban J, Sagawa H, Möller J, Murtagh DP, Mendrok J, et al. The level 2 research product algorithms for the Superconducting Submillimeter-Wave Limb-Emission Sounder (SMILES). Atmos Meas Tech 2011;4(10):2105–24. http://dx.doi.org/10.5194/amt-4-2105-2011.

Please cite this article as: Xu J, et al. Assessment of Tikhonov-type regularization methods for solving atmospheric inverse problems. J Quant Spectrosc Radiat Transfer (2016), http://dx.doi.org/10.1016/j.jqsrt.2016.08.003